EUROFUSION WPMST2-PR(16) 16462

L Piron et al.

Helical flow in RFX-mod tokamak plasmas

Preprint of Paper to be submitted for publication in Nuclear Fusion

This work has been carried out within the framework of the EUROfusion Consortium and has received funding from the Euratom research and training programme 2014-2018 under grant agreement No 633053. The views and opinions expressed herein do not necessarily reflect those of the European Commission.

Helical flow in RFX-mod tokamak plasmas

L. Piron[1], B. Zaniol[2], D. Bonfiglio[2], L. Carraro[2], A. Kirk[1], L. Marrelli[2], R. Martin[1], C. Piron[2], P. Piovesan[2], M. Zuin[2]
[1] *CCFE, Culham Science Centre, Abingdon, OX14 3DB, UK*
[2] *Consorzio RFX (CNR, ENEA, INFN, Università di Padova, Acciaierie Venete SpA),Corso Stati Uniti 4, 35127 Padova, Italy*
(Dated: October 6, 2016)

Abstract This work presents the first evidence of helical flow in RFX-mod $q(a) < 2$ tokamak plasmas. The flow pattern is characterized by the presence of convective cells with m = 1 and n = 1 periodicity in the poloidal and toroidal direction, respectively. A similar helical flow deformation has been observed in the same device when operated as a Reversed Field Pinch. In such plasmas, the flow dynamics was tailored by the innermost resonant m = 1, n = 7 tearing mode, who sustains the magnetic field configuration through the dynamo mechanism [Bonomo F. et al 2011 Nucl. Fusion 51 123007]. Instead, in the tokamak experiments presented here, it is strongly correlated with the m = 1, n = 1 MHD activity. A helical deformation of the flow pattern, associated with the deformation of the magnetic flux surfaces, is predicted by several codes, such as Specyl [Bonfiglio D. et al. 2005 Phys. Rev. Lett. 94 145001], PIXIE3D [Chacon L. et al 2008 Phys. Plasmas 15 056103], NIMROD [King J.R. et al. 2012 Phys. Plasmas 19 055905] and M3D-C1 [Jardin S.C. et al. 2015 Phys. Rev. Lett. 115 215001]. Among them, the 3D fully non-linear PIXIE3D has been used to reconstruct the 2D flow pattern. Inputs to the code are the modelled flow maps, the ion emission profiles as calculated by a 1D collisional radiative code [Carraro L. et al 2000 Plasma Phys. Control. Fusion 42 731], and a synthetic diagnostic with the same geometry installed in RFX-mod. A good agreement between the synthetic flow behavior and the experimental one has been obtained, confirming that the observed flow oscillations with the associated convective cells are a signature of helical flow.

I. INTRODUCTION

Plasma rotation in fusion devices can have a beneficial effect on plasma stability and confinement. For example, it is important to stabilize MHD modes, such as neoclassical tearing modes[1] and Resistive Wall Modes (RWM) [2]. Moreover, a plasma rotation shear is a key factor for turbulence suppression and the formation of transport barriers, which are important to achieve high-performance regimes [3]. In present day devices, a significant external momentum source can be provided by Neutral Beam Injection (NBI). However, in ITER and future reactors, NBI is not expected to provide much momentum. Consequently, other mechanisms of momentum injection have to be considered, for example those underlying intrinsic plasma rotation [4].

The RFX-mod experiment [5], when operated as a tokamak [6–8], can contribute to the study of the effects responsible for momentum injection and transport in absence of external heating systems in tokamak plasmas. In particular, thanks to the presence of a sophisticated feedback control system, made up of 192 active coils, independently driven and fully covering the torus surface, the effect of external 3D magnetic fields on plasma rotation can be investigated. In fusion experiments, external 3D magnetic fields can affect plasma rotation, since the NTV, JxB and the electromagnetic torques, which appear in the momentum balance equation, scale with the magnetic field amplitude [9]. Recent RFX-mod tokamak experiments have shown that the application of magnetic field perturbations in $q(a) < 2$ plasma regimes induce a braking or acceleration of plasma rotation, below or above a threshold of the applied radial magnetic field [10].

The novelty of the experiments reported in this paper is that, in the presence of rotating 3D magnetic fields, oscillations have been observed in the plasma flow, measured by the Doppler shift of spectral lines from several ion species. The flow oscillates at the same frequency of the MHD modes, which are maintened into rotation by the magnetic feedback [8, 11]. By correlating flow measurements with radial magnetic field data, $m = 1, n = 1$ (with m and n poloidal and toroidal mode numbers, respectively) convective cells have been inferred in the flow pattern, which are a signature of helical flow.

Helical magnetic structures from a theoretical point of view correspond to a magnetohydrodynamic minimum energy state accessed through a bifurcation process, characterized by an internal 3D helical magnetic equilibrium [12], featuring the same helicity as the experimental perturbation. For example, in RFX-mod tokamak experiments, it is associated with the internal $m/n = 1/1$ kink mode, which produces a helical distortion in the plasma core [13]. Instead, in Reversed Field Pinch (RFP) plasmas, helical equilibria are linked to the innermost resonant tearing mode, which sustains the magnetic field configuration [14, 15].

In this work, the first evidence of dynamo helical flow, associated with the internal 1/1 kink mode deformation, is presented. The presence of an helical flow in tokamak plasmas is predicted by several codes, such as Specyl [16],

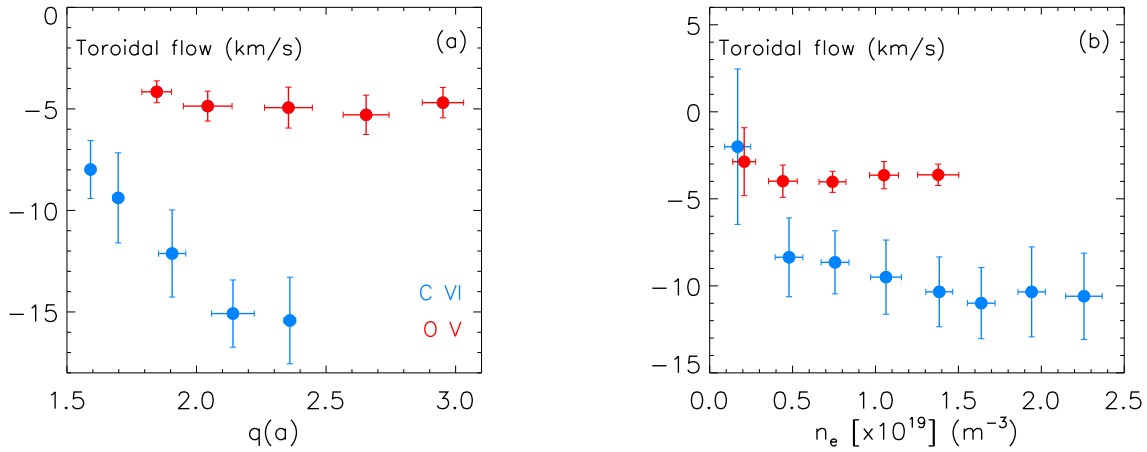

Figure 1: Toroidal C VI (in blue) and O V (in red) flow velocity as a function of (a) edge safety factor and (b) electron plasma density.

PIXIE3D [17], NIMROD [18] and M3D-C1 [19]. Among them, the 3D, fully non-linear PIXIE3D code, which has been extensively validated against RFX-mod tokamak plasmas [10, 13, 20], has been used to interpret the origin of the observed flow oscillations in combination with ad hoc 2D flow modelling code, which allows the reconstruction of rotation measurements.

Inputs to the 2D flow modelling are the PIXIE3D flow map, the ion radial emission profiles as calculated by a 1D collisional radiative code [21] and a synthetic passive spectroscopy diagnostic with the same geometry implemented in RFX-mod. The good agreement between the synthetic flow behavior and the experimental one demonstrates that the observed flow oscillations with the associated convective cells are a signature of helical flow. This confirms that the dynamo or magnetic flux pumping mechanism, and the associated helical flow, can sustain helical equilibria not only in high current RFP plasmas [15, 28, 30] but also in low-β RFX-mod tokamak plasmas and high-β DIII-D tokamak operations [32, 33].

The manuscript is structured as follows: in section II the interplay between plasma rotation and MHD activity will be presented with the main dependence of the plasma rotation on magnetic equilibrium and electron density. The evidence of flow oscillations in presence of externally applied magnetic field perturbations will be described in section III. In section IV the results of the 2D flow modelling code will be compared with experimental flow behavior. The summary and conclusions of this work are given in section V.

II. INTERPLAY BETWEEN PLASMA ROTATION AND MHD ACTIVITY

The RFX-mod device has been operated as a circular tokamak, exploring magnetic equilibria with $q(a) < 2$ and $q(a) > 2$ in different density regimes. The behaviour of plasma rotation in such plasmas has been studied using data from a multi-chord Doppler spectroscopic diagnostic based on line-of-sight (los) integrated emissivity measurements of different ion stages. In particular, emissions from C VI, ($\lambda = 5290\mathring{A}$), the main impurity coming from the graphite first wall, and O V, ($\lambda = 6500\mathring{A}$), have been statistically characterized in standard discharges, without magnetic field perturbations.

The reconstruction of the ion emissivity profiles is obtained by a 1D collisional radiative impurity transport code. The simulations have been performed considering coronal, no-transport, and high impurity transport regimes characterized by the transport coefficients $D = 20m^2s^{-1}$ and v as in [21]. A scan on diffusion coefficient and pinch velocity in the impurity transport equations has shown that independently from the hypothesis on the transport regime, the C VI emissivity is rather spread over the minor radius with a broad peak centered around mid radius, $r/a \approx 0.35$. Instead, the O V emissivity is relatively sharply peaked near the edge, $r/a \approx 0.8$.

Rotation measurements from such ion emissions show that the intrinsic rotation in RFX-mod is mainly influenced by the edge safety factor, as reported in Fig.1(a). This is similar to what has been observed in TCV Ohmic discharges [22]. Note that the intrinsic rotation in RFX-mod tokamak plasma is in counter-I_p direction (negative values). Differently from rotation scaling results obtained in Alcator C-mod experiment [23], no velocity reversal occurs below a threshold value of plasma density, as highlighted in Fig.1(b). In future RFX-mod experimental campaigns, the role

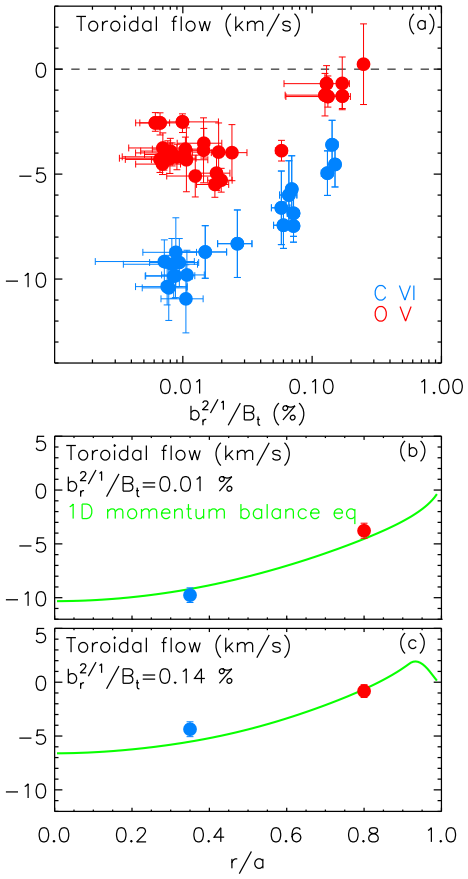

Figure 2: (a) Toroidal rotation as a function of $b_r^{2/1}/B_t$ for two sets of similar $q(a) < 2$ tokamak discharges. The blue dots correspond to data from C VI emission, the red ones from O V. (c-d) Radial profile of the toroidal rotation, solution of the 1D momentum transport model described in [10], in the absence of 2/1 magnetic field perturbations applied ($b_r^{2/1}/B_t \approx 0.01\%$) and in presence of it ($b_r^{2/1}/B_t \approx 0.14\%$), respectively. The dots correspond to the mean value of rotation measurements from CVI and OV emission for the normalized 2/1 radial magnetic field amplitudes reported above.

of collisionality in producing the flow inversion [9] will be further investigated by dedicated experiments.

Interestingly, a significant change of toroidal plasma rotation has been observed in presence of MHD modes. In the following subsections, the plasma rotation behavior in presence of the 2/1 RWM and the 2/1 TM is presented.

Plasma rotation in presence of 2/1 RWM

In RFX-mod $q(a) < 2$ tokamak plasmas, the 2/1 RWM can be controlled by the active feedback system, by zeroing the associated radial magnetic field, or can be kept at a finite amplitude by setting a finite reference value on the 2/1 radial magnetic field, that could be rotated at a selected frequency or maintained static. In this work the second technique has been applied to investigate the plasma rotation dynamics, in presence of a 2/1 RWM with a finite radial magnetic field. Several experiments with similar plasma parameters have been performed by applying various amplitudes of the external 3D magnetic field, rotating with $10Hz$ frequency.

Fig.2(a) shows the toroidal C VI (blue) and O V (red) flow velocity as a function of the 2/1 edge radial magnetic field amplitude normalized to the equilibrium field, $b_r^{2/1}/B_t$, for plasmas with $q(a) \approx 1.7$ and $n_e = 1$ to 2.5 x $10^{19} m^{-3}$.

First investigations reported in [10] showed that C VI decelerates as soon as the amplitude of the 2/1 RWM increases. Also the new O V flow data, referred to a more external radial position, follow the same trend. This rotation behavior appears to depend on the 2/1 RWM amplitude only, since in the set of analyzed discharges similar plasmas have been chosen.

The rotation braking is dictated by the stochastic force, associated with the presence of an ambipolar electric field

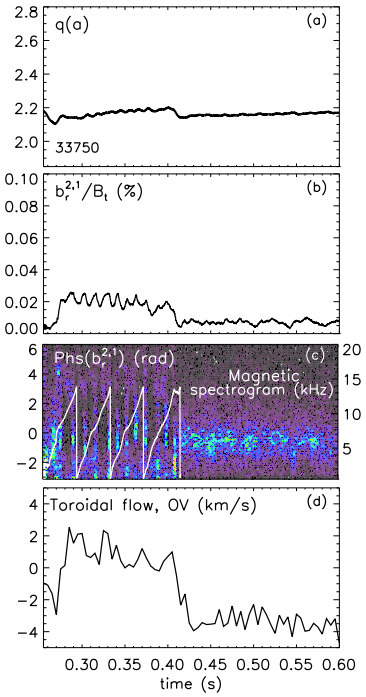

Figure 3: Time behaviour of (a) the edge safety factor, (b) the normalized radial magnetic field amplitude of the 2/1 TM and (c) the corresponding phase, together with the magnetic spectrogram which shows the mode behavior in the fast frequency branch, and (d) toroidal O V flow velocity.

in the plasma edge, as described by a 1D momentum transport model, taking into account the mechanisms that can play a role in such plasmas, such as the neoclassical toroidal viscosity, the stochastic force, and the friction force due to neutrals coming from the wall [10].

By combining toroidal C VI flow velocity data with the O V ones, information on the toroidal rotation profile can be gathered, since such ions are localized far apart along the radius, as obtained by the impurity code. The radial profiles of the toroidal flow, solutions of the 1D momentum transport model without and with externally applied magnetic field perturbations are plotted in Fig.2(b-c) with a green line, respectively. On the same figure, the mean toroidal C VI and O V flow velocities are indicated with circles. A good agreement between the 1D momentum transport model and the experimental data has been obtained, confirming that the model, despite of its simplicity, is able to capture the physical mechanisms which govern plasma rotation in presence of a 2/1 RWM.

Plasma rotation in presence of 2/1 tearing mode

In $q(a) > 2$ tokamak plasmas, a 2/1 rotating TM is present, which can transit from the fast rotation branch (some kHz) to the slow one (some Hz, as imposed by feedback control system), depending on the amplitude of the radial magnetic field at the resonant surface, as predicted theoretically in [24]. The plasma rotation is affected by the 2/1 TM dynamics when it rotates in the slow frequency branch, therefore when it has a non-negligible amplitude.

An example of the interplay between toroidal rotation and 2/1 TM is reported in Fig.3. This figure shows the time behavior of the edge safety factor, the normalized radial magnetic field amplitude of the 2/1 TM and the corresponding phase and frequency, from a fast magnetic field signal, and the O V toroidal velocity.

As the magnetic equilibrium is approaching the $q(a) = 2$ resonance, the 2/1 TM increases in amplitude. In this case, it rotates in the slow frequency branch, at around 25Hz, as shown in panel (c) of the figure, and the plasma rotation is nearly 1.5km/s in co-I_p direction. As soon as the mode decreases in amplitude, probably due to modifications in the equilibrium profile, at around t = 0.4s, it jumps to the fast rotation branch, rotating at 5kHz, and the plasma rotates in counter-I_p direction at 4km/s. In this experiment, the electron magnetic torque, induced by the presence of a localized singular current in the vicinity of the 2/1 resistive layer [25, 26], is responsible for the change in the plasma rotation direction.

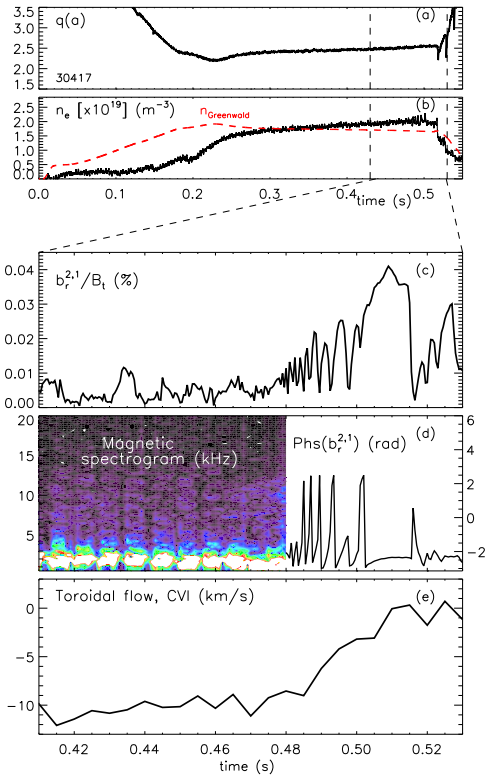

Figure 4: Time behaviour of (a) the edge safety factor, (b) electron density, in black, and calculated Greenwald density, in red, (c) the normalized radial magnetic field amplitude of the 2/1 TM, and (d) the corresponding phase, together with the magnetic spectrogram, and (e) toroidal C VI flow velocity.

Instead, in experiments at high density, near the Greenwald density limit, it has been observed that the plasma rotation always brakes due to the presence of a locked 2/1 TM and the plasma disrupts. In the experiment reported in Fig.4, before t = 0.48s, a 2/1 TM is rotating in the fast frequency branch, at f = 2kHz, as shown in Fig.4(d). As the plasma approaches the density limit, reported in red in panel (b) in the same figure, the 2/1 TM slows down, increasing in amplitude, up to a time instant in which the plasma rotation brakes, as shown in panel (e), and a plasma disruption is triggered. Also in this case, the plasma rotation drops, during mode locking phase, is mainly governed in the momentum transport balance by the electromagnetic torque, whose amplitude is increasing since the size of the 2/1 TM island is getting larger when approaching the density limit.

These $q(a) > 2$ experiments confirm the existence of a strict relation between the TM activity and plasma rotation in RFX-mod. A similar connection has been observed for the 2/1 RWM case, as described in the previous subsection, even if the mechanisms governing the momentum transport are different.

III. CHARACTERIZATION OF HELICAL FLOW

Rotating 3D magnetic fields force flow oscillations

As reported in the previous Section, the 2/1 RWM in $q(a) < 2$ plasmas can be maintained at fixed amplitude, by applying rotating 3D magnetic fields. In this kind of experiments, in addition to a reduction of toroidal flow, time-oscillations in toroidal flow measurements have been observed.

Fig. 5, on the left hand side, shows the time behavior of edge safety factor, the normalized radial magnetic field amplitude of the 2/1 RWM and the toroidal O V velocity for 4 $q(a) < 2$ experiments in which 2/1 magnetic perturbations with increasing amplitude, rotating at 10Hz frequency, have been applied by means of the active control system. Here, the color code has been used to distinguish different amplitudes of the applied perturbation.

Fig. 5(c) shows that in these experiments the toroidal rotation can either oscillate, like in the blue and green cases,

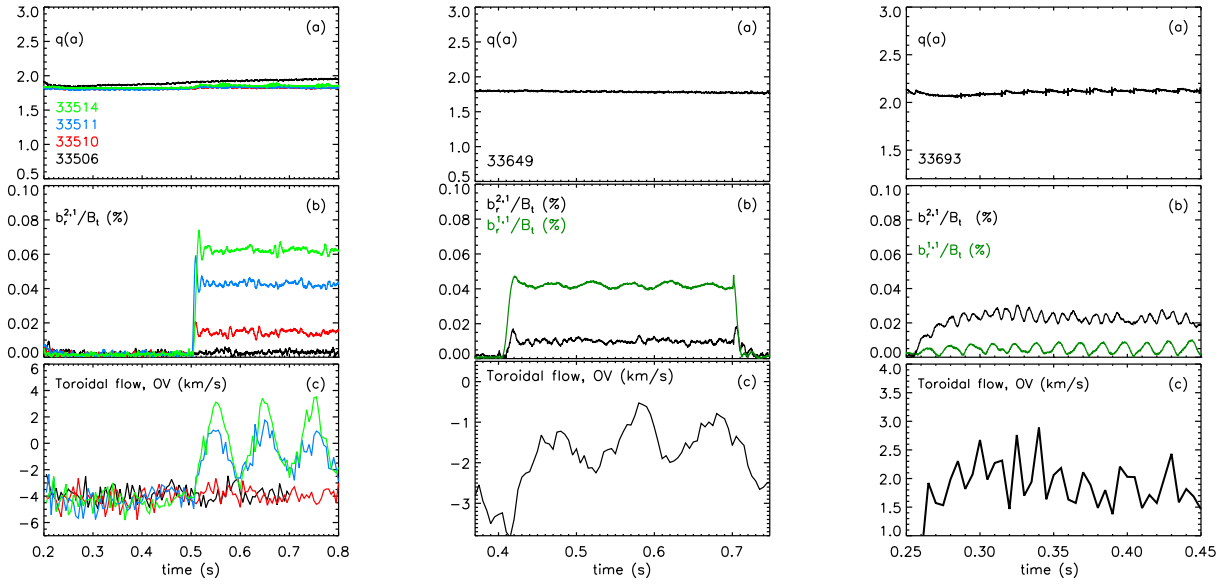

Figure 5: Time behaviour of (a) the edge safety factor, (b) the normalized radial magnetic field amplitude of the 2/1 RWM and (c) toroidal O V flow velocity. On the left side: $q(a) < 2$ plasma experiments in which a rotating 2/1 RWM is kept at finite amplitude, rotating at $f = 10Hz$, by externally applied 2/1 magnetic field perturbations at increasing amplitude (different colours). In the centre: $q(a) < 2$ plasma experiment in presence of an externally applied 1/1 magnetic field perturbation, rotating at $f = 10Hz$. On the right side: $q(a) > 2$ plasma experiment where a 2/1 TM is forced to rotate at $f = 25Hz$ by an externally applied 2/1 magnetic field perturbation.

or stay constant, like in the red one, depending on the amplitude of the applied magnetic field. The flow oscillations appear above a threshold $B_r^{2,1}/B_t$ which is around 0.04%. It is noteworthy that the frequency of these oscillations corresponds to the one of the externally applied field.

Plasma rotation is induced to oscillate not only in presence of 2/1 but also with rotating 1/1 3D magnetic fields, as shown in Fig. 5, on the center. In this case, as reported in panel (b) of the figure, the amplitude of the 1/1, shown in green, is kept at finite amplitude and rotating at 10Hz. Since a 2/1 sideband is induced by toroidal coupling, also the 2/1 RWM has finite amplitude. Similar to the previous case, the toroidal flow oscillates at the same frequency of the 1/1 internal kink mode, or of the 2/1 RWM, which are both forced to rotate by the external perturbation.

Rotating 2/1 magnetic field perturbations have been applied also in $q(a) > 2$ plasmas, in presence of a 2/1 TM. Fig. 5, on the right hand side represents an example. In particular, the figure shows the time behavior of edge safety factor, the normalized radial magnetic field amplitude of the 2/1 TM and the flow measurement from O V emission of a $q(a) = 2.1$ experiment in which a 3D magnetic field, rotating at 25Hz, has been applied. In this case, the 2/1 TM has a relatively large amplitude and therefore it is forced by magnetic feedback to rotate in the slow frequency branch, at 25Hz. Toroidal flow oscillations are correlated with the 2/1 mode rotation, as shown in panel (c) of the figure.

In summary, whenever the MHD mode is forced to rotate by magnetic feedback control (2/1 RWM or 2/1 TM), toroidal flow oscillations can be observed. Though the examples reported here characterize the behavior of O V toroidal flow, similar oscillations have been observed also in data from different ions, as will be discussed below.

Hints of m=1 and n=1 convective cells in flow pattern

Measurements of different impurity spectral lines from C VI, C V , O V and C III, have been collected in $q(a) < 2$ plasmas and in presence of a 2/1 RWM, maintained at constant amplitude and rotating at slow frequency, by means of 3D magnetic fields. Such measurements allow us to gather information on the effect of the 2/1 external magnetic field perturbation on plasma rotation at different radial positions: C VI and C V in the core, and O V and C III at the plasma edge. The radial localization of the different ion impurities, predicted by the 1D collisional radiative code described in Section 1, is reported in Table 1.

Toroidal flow deduced from different ions is reported in Fig. 6, which shows on the top panels (a,b,c,d) the time behavior of the edge safety factor of 4 similar plasma experiments and on the bottom ones (d,e,f,g) plasma rotation

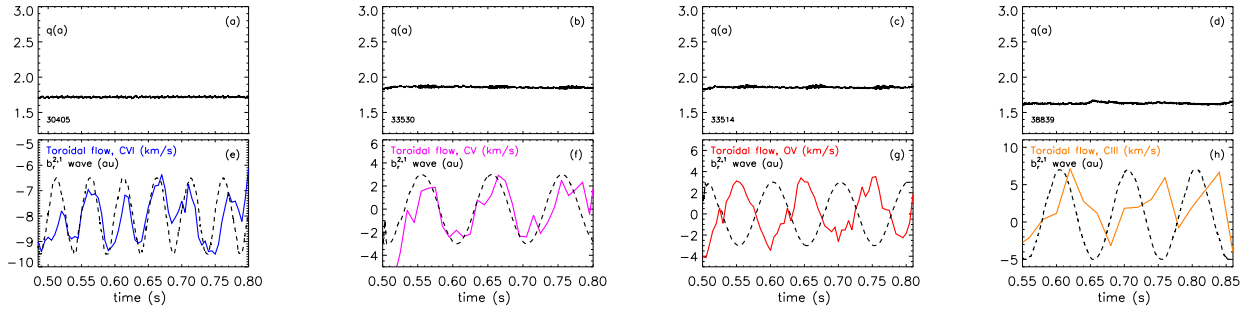

Figure 6: Time behaviour of (a, b, c, d) the edge safety factor and (e, f, g, h) toroidal C VI, C V, O V and C III flow velocity, respectively. The dotted line corresponds to the 2/1 radial magnetic field fluctuation. In all the experiments, the 2/1 RWM is kept at fixed amplitude and slowly rotating by an externally applied 2/1 magnetic field perturbation.

Ion	Radial location (r/a)
C VI	0.35 ±0.5
B V	0.47 ±0.5
C V	0.56 ±0.5
B IV	0.76 ±0.5
O V	0.81 ±0.5
C III	0.87 ±0.5
B II	0.91 ±0.5

Table I: Radial localization of the different ion impurities, calculated using the 1D collisional radiative code described in the text. B II, B IV velocity data are not present in RFX-mod but they are reported here since they have been simulated by the 2D flow modelling code, described in Section IV.

measurements inferred from C VI, C V , O V and C III, respectively. The dotted line superimposed on the flow data corresponds to the 2/1 radial magnetic field fluctuation.

In all these experiments, independently on the ion emission, plasma rotation oscillates with the same frequency of the 2/1 radial magnetic field. In particular, while C VI and C V flows show oscillations in phase with the 2/1 radial magnetic field fluctuations, O V and C III are in phase opposition. Therefore, in the plasma center, the flow oscillates in one direction, at the edge in the opposite one. The observed inversion of the flow oscillations, together with the evidence that the plasma is forced to rotate as the applied n=1 magnetic field, or the 2/1 RWM, suggests the presence of n=1 convective cell in the toroidal flow pattern.

Spectroscopic data are also available for the poloidal rotation in RFX-mod. Different from the toroidal component, poloidal flow could be derived only from the intense line emission of C V ($\lambda = 2271\mathring{A}$) and has low amplitudes, around $2kms^{-1}$, likely due to neoclassical poloidal flow damping [27]. In future RFX-mod tokamak operations, a doped pellet injector will be used in order to produce stronger emission lines allowing the study of the poloidal flow behavior at different radial positions.

C V poloidal flow measurements are available both in the high field side (HFS) and low field side (LFS) of the plasma, along lines of sight as plotted in Fig. 10, on the right.

The effect on poloidal rotation of an externally applied 2/1 3D magnetic field, rotating at 10Hz, is shown in Fig.7.

The amplitude of the external perturbation is not constant in time, as in the experiments reported before, but it increases, from t = 0.3 - 0.55s, and then decreases from t = 0.55 - 0.8s. The 2/1 RWM and the 1/1 internal kink mode, whose dynamics are reported in Fig.7(b-c), are affected by the external magnetic field: their amplitude follows the triangular shaped perturbation, and their frequency is the same as the one imposed by the feedback control system.

The poloidal flow measured by a line of sight located in the HFS (in blue) shows the same time behavior as the LFS one (in red), as reported in Fig.7(d). In presence of an oscillating m=1 structure in the poloidal flow pattern, as plotted in the sketch in Fig.8, similar flow signals should be detected by two lines of sight mirror-like with respect to a vertical diameter. Instead, in presence of an oscillating m=0 structure, which implies a rotation around the poloidal angle, the two lines of sight should detect flow signals oscillating in anti-phase. Since the time behaviour of the HFS and LFS poloidal flow signals are very similar in phase, a m=1 structure in the poloidal flow map could be present. In order to eliminate the even components in the poloidal flow, the difference of the flow measurements reported in

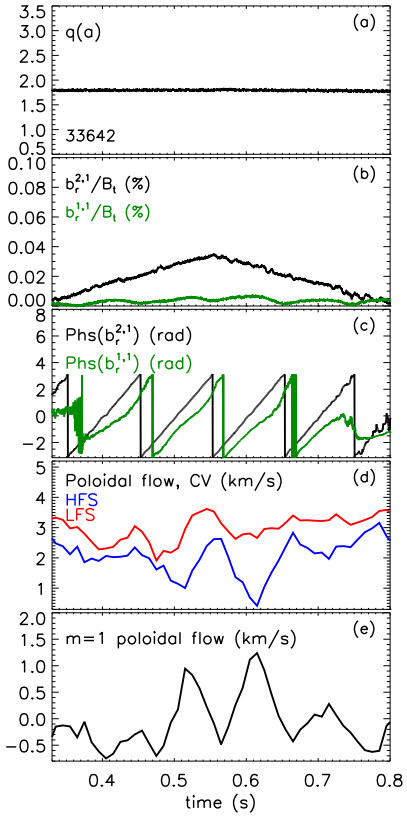

Figure 7: Time behaviour of (a) the edge safety factor, (b-c) the normalized radial magnetic field amplitude and the corresponding phase of the 2/1 RWM (in black) and 1/1 internal kink mode (in green) (d) poloidal CV flow velocity as measured in the HFS (in blue) and in the LFS (in red) and (e) m=1 poloidal flow component of a $q(a) < 2$ plasma experiment in which a 2/1 triangular shaped magnetic field perturbation, rotating a $10Hz$, is applied through magnetic feedback.

Fig.7(d) has been calculated and this quantity is reported in Fig. 7(e). Despite the amplitude of the oscillations is small, around 1km/s, the time behavior of such odd contributions to the flow are correlated with the 1/1 internal kink mode dynamics. Instead, the even contributions do not show any correlation. This evidence might suggest the presence of a m=1 convective cell.

Because n=1 and m=1 convective cells have been observed in velocity data, we can therefore speculate that the plasma rotation is helically tailored. Such flow distortion has been observed in presence of 2/1 or 1/1 externally applied magnetic field perturbations since in such situation the internal 1/1 kink mode amplitude and the associated flux surface deformation is larger than in standard plasmas, without externally applied magnetic field perturbations.

In these plasmas, the flow can play a role in the formation and sustainment of the helical equilibrium, as described in [13]. This is very similar to what has been observed in RFP configuration, both in RFX-mod and MST devices, where the helical flow is linked to the innermost resonant TM [28–30].

IV. MODELLING OF HELICAL FLOW PATTERN

The existence of a helical dynamo velocity field associated with the helical deformation of the magnetic surfaces has been predicted in several codes [16–19]. The 3D, fully non-linear PIXIE3D code, already used in [10] to understand the physical mechanisms ruling the momentum transport in presence of 2/1 RWM, has been applied to predict the flow pattern, which has been given as input to a 2D flow modelling code.

Such code calculates synthetic flow measurements using a diagnostic geometry similar to the RFX-mod one, and the ion emission profiles calculated by the 1D collisional radiative code. This tool has allowed the understanding of the nature of the flow oscillations experimentally observed.

In particular, PIXIE3D simulations considered in this work used on-axis Lundquist number $S = 3$ x 10^4, Prandtl

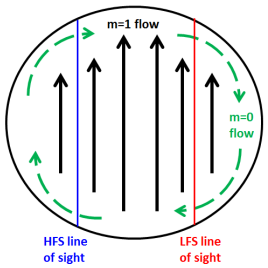

Figure 8: m=1 (black arrows) and m=0 (green dashed arrows) flow pattern in a toroidal cross section. The vertical lines represent lines of sight in the HFS (in blue) and in LHS (in red).

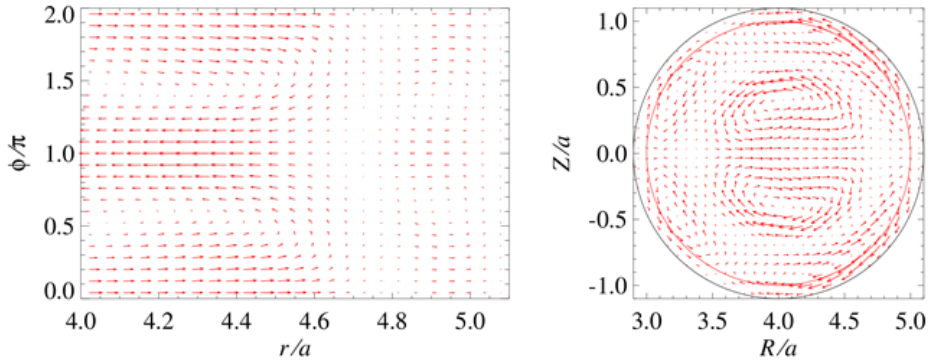

Figure 9: (a) Toroidal and (b) poloidal flow map from PIXIE3D RFX-mod tokamak simulation with $q(a) = 1.9$ in presence of $b_r^{2/1}/B_t \approx 0.1\%$ magnetic field perturbation.

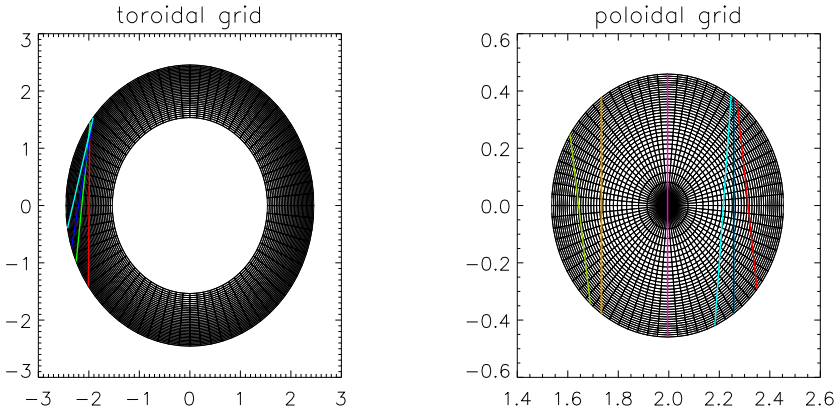

Figure 10: Toroidal (on the left) and Poloidal (on the right) cross sections with fine grids and lines of sight geometry used in the 2D modelling flow code.

number P = 3, aspect ratio R/a = 4, initial axisymmetric equilibrium with $q(0) = 0.8$, $q(a) = 1.9$, and current density profile of the form $j_\phi = j_0(1 - (r/a)^2)^\nu$ where $\nu = q(a)/q(0) - 1$, as in [10]. A vacuum region between the plasma boundary (r = a), which ideally corresponds to the position of the graphite tiles in RFX-mod, and the wall (r/a = 1.1) is modelled by a region of large resistivity. The presence of a 2/1 3D magnetic field in PIXIE3D is modelled adding to the wall, which behaves as an ideal shell, a fixed helical component with 2/1 helicity.

A normalized 2/1 magnetic field perturbation with relatively large amplitude, of about 0.1%, has been considered in order to highlight the effect of the 2/1 magnetic field perturbation on the plasma dynamics. When applying such perturbation, due to the toroidal coupling, also the dynamics of the 1/1 internal kink mode is affected. Experimentally in presence of external 2/1 magnetic fields, it has been observed that the sawtooth period and amplitude decrease

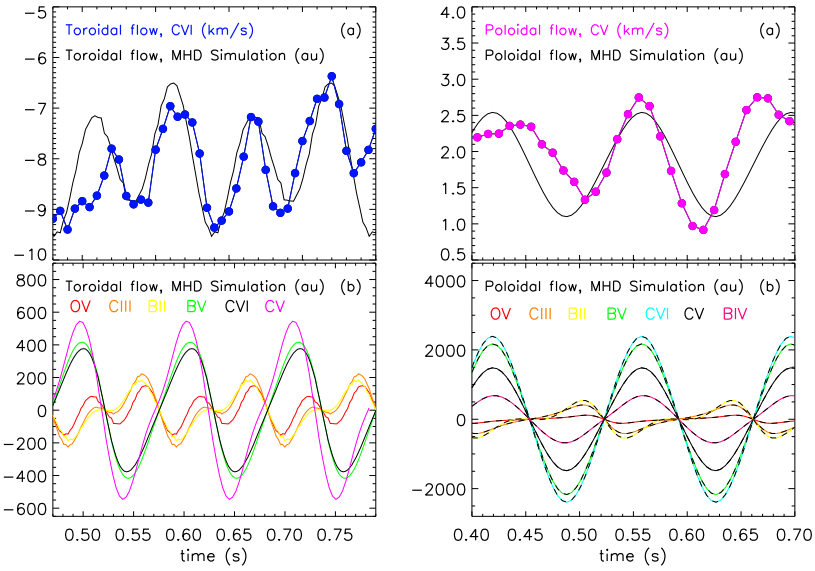

Figure 11: On the left: (a) Time behaviour of toroidal C VI velocity from 30405 experiment (blue dots) and from PIXIE3D simulation (black line), (b) time behaviour of toroidal flow velocity of multiple ion species, predicted by PIXIE3D code. The signals correspond to a line of sight in the poloidal plasma cross section with impact parameter $\rho/a = 0.4$. On the right: (a) Time behaviour of poloidal C V velocity from 33642 experiment (magenta dots) and from PIXIE3D simulation (black line) (b) time behaviour of poloidal flow velocity of multiple ion species, predicted by PIXIE3D code. The signals correspond to two lines of sight, with impact parameter $\rho/a = 0.2$, mirror-like with respect to the vertical diameter. The line of sight in the HFS is represented with a solid line, the one in the LHF with a dashed line. Different colours have been used to distinguish various ions flow velocity.

and a stationary 1/1 helical equilibrium forms. The code is able to describe such dynamics, as documented in [13].

The flow pattern predicted by a PIXIE3D simulation is reported in Fig. 9(a,b) in a poloidal and toroidal plasma cross section, respectively. The result suggests the presence of m=1, n=1 convective cells associated with the helical deformation due to the internal 1/1 kink mode, which is mainly localized in the plasma core, and m=2, n=1 convective cells at the position of the wall. The 2/1 convective cells appear since the 2/1 external kink develops and non-linearly saturates in the simulation with radial profile consistent with the 2/1 imposed helical boundary condition.

In order to model the flow pattern and reconstruct the measurements, a 2D flow modelling code has been developed. The 2D flow modelling code divides the PIXIE3D flow map in fine elements, i.e. cells. For each of them a vector has been assigned. The components of the vector correspond to the toroidal and poloidal flow component, $\mathbf{v}(\mathbf{x})$. For each cell, also a value of ion emissivity, ξ^{ion}, is ascribed.

The flow measured along a line of sight, for a certain ion can be written as $< v_{los}^{ion} >= \int_{los} \xi^{ion}(\mathbf{x})\mathbf{v}(\mathbf{x}) \cdot d\mathbf{x} / \int_{los} \xi^{ion}(\mathbf{x})d\mathbf{x}$. To calculate the mean flow along the line of sight, the following expression has been used $< v_{los}^{ion} > \cong \sum_{i-cell} \xi_i^{ion}(\mathbf{v} \cdot \widehat{los})_i l_i / \sum_{i-cell} \xi_i^{ion} l_i$, where l_i represents the lenght of the line of sight inside the i-cell.

Fig.10(a,b) show the fine grids and the geometry of the lines of sight used for the synthetic flow measurement calculation, in the poloidal and toroidal cross section, respectively. The time evolution of the plasma flow has been reconstructed by simply rotating the lines of sight for the toroidal case, instead considering sections at different toroidal angles, for the poloidal one.

A comparison between the reconstructed toroidal C VI flow velocity and the experimental one for a chord with impact parameter $\rho/a = 0.4$, indicated in red in Fig. 10(a), is shown in Fig.11(a) on the left. In the synthetic flow measurement, highlighted with a black line, oscillations can be detected which are due to the rotating 1/1 mode. Therefore, the flow oscillations observed in the experimental data are allied with n=1 internal kink mode which is forced to rotate by the external magnetic field perturbation.

Moreover, synthetic flow measurements, detected by the same line of sight and calculated from the emission of different ion species, show that toroidal core flow velocity oscillates in opposite phase with respect to toroidal edge flow velocity, as reported in Fig.11(b) on the left. This behaviour is similar to what has been observed experimentally: the toroidal C V and C VI flow velocity oscillates in phase with the 2/1 radial magnetic field, instead, the flow rotation from edge ions, i.e. O V and C III, oscillates in opposite phase, as shown in Fig.6. Based on such agreement between the model predictions and the experimental data, it is possible to conclude that a n=1 convective cell is present in

the toroidal flow map.

A similar comparison has been carried out for the poloidal component of the plasma rotation. Fig.11(a) on the right shows the time behaviour of the poloidal C V flow velocity from experimental data, reported with magenta dots, and the synthetic flow measurement, plotted with a black line, as detected by a chord located in the LFS, with impact parameter $\rho = 0.2$. Such chord is shown in blue in Fig. 10(b). A good agreement between the experimental flow behaviour and the synthetic one has been obtained, demonstrating that, the poloidal flow modulation is linked to the dynamics of the internal 1/1 kink mode.

In addition to this, synthetic poloidal flow measurements have been reconstructed for a chord in the HFS with the same impact parameter as in the LFS. The time behavior of such poloidal HFS and LFS synthetic measurements are shown in Fig.11(b) with solid and dashed lines, respectively. Different colors have been used to distinguish various ions flow velocity. Independently of the ion analyzed, HFS poloidal flow has the same time behavior as in the LFS. This is consistent with the experimental data reported in Fig.7(d), leading to the conclusion that a m=1 component is present in the experimental flow pattern.

Similar to what has been observed for the synthetic toroidal flow measurements from different ion species, the poloidal flow velocity in the core oscillates with opposite phase with respect to the edge one, as reported in Fig.11(b) on the right. Since only poloidal C V flow velocity data are currently available in RFX-mod a direct comparison of flow behavior from different ions cannot be performed. The 2D modelling code suggests that C VI and B IV velocity oscillations have larger amplitude with respect to edge ions, such as O V, C III or B II. Measurements from such ions in future RFX-mod experiments will allow to confirm the presence of a m=1 convective cell.

The good agreement between the synthetic flow behavior and the experimental one, confirms that the flow oscillations, with the associated convective cells, are a signature of helical flow. It is worth mentioning that the comparison can be presently done only on a qualitative basis. Indeed the present version of PIXIE3D neglects any momentum source in the momentum balance equation, both in the toroidal and poloidal directions. Furthermore, the code assumes the same phase for all the modes, therefore the mean electromagnetic torque is null as well. These assumptions can lead to a prediction of the flow values larger than the experimental ones. A detailed investigation on this issue is beyond the scope of the work and it will be addressed in a future paper.

V. CONCLUSIONS

In this work, the intrinsic rotation in RFX-mod tokamak plasma has been characterized, with and without the application of 3D magnetic field perturbations. Without perturbations, plasma rotation depends on the magnetic equilibrium, but not on the electron density. This is different from Alcator-C Mod results which show a flow inversion above a threshold value of the electron density [9].

The presence of magnetic field perturbations, due to MHD activity or external feedback currents, strongly affects the plasma rotation. It has been observed that the plasma rotation in $q(a) < 2$ plasmas, decelerates when the normalized radial magnetic field amplitude of the 2/1 RWM, kept at finite amplitude by means of an externally applied 3D field, is around 0.02%. The same is observed in high density regimes, when a 2/1 TM, in $q(a) > 2$ plasmas, locks. However, the mechanism governing the plasma rotation braking is quite different in such experiments. In presence of a 2/1 RWM the stochastic force, due to the presence of an ambipolar electric field at the plasma edge, plays a major role in the momentum balance equation [10], instead in presence of a 2/1 TM the electromagnetic force is expected to be the most important term [25, 26].

In presence of external 3D magnetic fields, flow oscillations have been observed, which are correlated with the MHD activity. These oscillations have been detected in $q(a) = [1.8, 2.1]$ plasmas. In this paper, experimental analysis of flow oscillations, and the corresponding modelling, has been presented for plasmas with $q(a) < 2$.

Toroidal flow oscillations appear in plasmas with normalized radial magnetic field amplitude above a threshold value, around 0.04%, and have been observed both in the core flow velocity, as shown by C V and C VI data, and in the edge one, as indicated by O V and C III. In particular, the toroidal flow oscillates in phase with the 2/1 RWM mode, in the core. Instead it oscillates in antiphase, at the edge. This can be the signature of a n=1 convective cell in the toroidal flow map.

The poloidal component of plasma rotation exhibits low amplitude oscillations, of about 1km/s, in presence of rotating magnetic field perturbations. Lines of sight mirror-like with respect to the vertical diameter show the same flow time dynamics, and by neglecting the even components in such measurements, m=1 flow oscillations have been observed which are correlated with the internal 1/1 kink mode activity. These evidences can be hints of a m=1 convective cell in the poloidal flow pattern.

The presence of m=1, n=1 convective cells in the flow map has been investigated by developing a 2D flow modelling code which can reconstruct synthetic flow measurements from the PIXIE3D code flow map, a diagnostic with a geometry similar to the experimental one, and ion emission profiles as obtained by the 1D collisional radiative code.

The 3D, fully non-linear PIXIE3D code in presence of external 3D magnetic fields, in fact, predicts the existence of a ExB flow associated with the helical deformation of the flux surfaces, which are due mainly to the 1/1 mode in the core and to the 2/1 one at the plasma wall. The latter mode, which has a TM nature, is induced by the imposed helical boundary condition. A good agreement between synthetic flow measurements and experimental results has been obtained, confirming that the oscillations, observed in toroidal and poloidal velocity data, are a signature of helical flow.

Such evidence, supported by SXR core data, which shows the presence of a 1/1 stationary helical equilibrium in presence of externally magnetic field perturbations, as described in [13], implies that an helical equilibrium sustained by the dynamo mechanism can be present in RFX-mod tokamak plasmas. Helical equilibria have been observed in the same device when operated as a RFP exploring high current regimes [36] and in the MST RFP experiment [30], and they are sustained by the innermost resonant TM. In the tokamak experiments analyzed here, helical equilibria are associated with the internal 1/1 kink mode.

A helical flow linked to magnetic flux surfaces deformation is predicted by several codes [16–19]. In this work, it has been experimentally demonstrated for the first time in a tokamak plasma, performing a validation between the flow measurements and the synthetic ones, calculated with the 2D flow modelling code. This can support the idea that the dynamo or flux-pumping mechanism can sustain helical states not only in high current RFP and low-β RFX-mod tokamak plasmas but also high-β hybrid tokamak operations as described in [19, 32, 33].

VI. ACKNOLEDGMENT

The author is grateful to L. Chacón for providing the PIXIE3D code and valuable comments. This work has been carried out within the framework of the EUROfusion Consortium and has received funding from the Euratom research and training programme 2014-2018 under grant agreement No 633053. The views and opinions expressed herein do not necessarily reflect those of the European Commission. This project has also received funding from the RCUK Energy Programme [grant number EP/I501045]. To obtain further information on the data and models underlying this paper please contact PublicationsManager@ccfe.ac.uk.

[1] La Haye R.J. et al 2010 *Phys. Plasmas* **17** 056110
[2] Chu M.S. and Okabayashi M. 2010*Plasma Phys. Control. Fusion* **52** 123001
[3] Burrell K. H. 1998 *Science* **281** 1816
[4] Rice J. E. et al. 2007 Nucl. Fusion 47 1618
[5] Sonato P. et al 2003 *Fusion Eng. Des* **66** 161
[6] Martin P. et al 2011 *Nucl. Fusion* **51** 094023
[7] Baruzzo M. et al 2012 *Nucl. Fusion* **52** 103001
[8] Zanca P. et al 2012 *Plasma Phys. Control. Fusion* **54** 094004
[9] Rice J. E. et al. 2016 Plasma Phys. Control. Fusion **58** 083001
[10] Piron L. et al 2013 *Nucl. Fusion* **53** 113022
[11] Zanca P. et al 2015 *Nucl. Fusion* **55** 043020
[12] Cooper W. A. et al. 2010 *Phys. Rev. Lett.* **105** 035003
[13] Piron C. et al 2016 *Nucl. Fusion*
[14] Lorenzini R et al 2009 *Nature Physics* **5** 570
[15] Bergerson W. F.et al 2011 *Phys. Rev. Lett.* **107** 255001
[16] Bonfiglio D. et al. 2005 *Phys. Rev. Lett.* **94** 145001
[17] Chacón L. et al. 2008 *Phys. Plasmas* **15** 056103
[18] King J.R. et al. 2012 *Phys. Plasmas* **19** 055905
[19] Jardin S.C. et al. 2015 *Phys. Rev. Lett.* **115** 215001]
[20] Bonfiglio L. et al 2015 *Plasma Phys. Control. Fusion* **57** 044001
[21] Carraro L. et al 2000 *Plasma Phys. Control. Fusion* **42** 731
[22] Scarabosio A. et al 2006 *Plasma Phys. Control. Fusion* **48**) 663
[23] Rice J.E. et al 2011 *Nucl. Fusion* **51** 083005
[24] Fitzpatrick R. *1999 Phys. Plasmas* **6** 1168
[25] Nave M. F. et al 1990 *Nucl. Fusion* **30** 2575
[26] Yokoyama M. et al 1996 *Nucl. Fusion* **36** 1307
[27] Helander P. and Sigmar D.J. 2000 *Collisional Transport in Magnetized Plasmas* (Cambridge: Cambridge University Press)
[28] Piovesan P. et al 2004 *Phys. Rev. Lett.* **93** 235001
[29] Piovesan P. et al 2011 *Plasma Phys. Control. Fusion* **53** 084005
[30] Bonomo F. et al 2011 *Nucl. Fusion* **51** 123007

[31] Wesson J. et al 1978 *Nucl. Fusion* **18** 87
[32] Luce T.C. et al 2014 *Nucl. Fusion* **54** 013015
[33] Piovesan P. et al 2016 *IAEA Proceeding Role of MHD dynamo in the formation of 3D equilibria in fusion plasmas* 26th IAEA Fusion Energy Conference, 17-22 October 2016, Kyoto, Japan Kyoto, Japan